SURVEY OF ORAL CANCER PREDICTION METHODS

Keerthinathan, Meka Kavya Uma Meghana, Lavanya Gopinath,

Sheba Sulthana and Vishal Krishh

Department of Artificial Intelligence Engineering, Amrita Vishwa Vidyapeetham,

Chennai Campus

ABSTRACT:

Oral cancer has been one of the most mortal diseases in the world, and accurate and timely treatment will efficiently improve the survival and cure rate of the patients. However, the traditional diagnosis ways by the clinicians could be laborious and easily misdiagnosed, and oral cancer usually with different morphological features, which makes it challenging to achieve the high accuracy classification automatically. To address this challenge, in this paper, we classified the various types of oral cancer detection using various advance techniques around the world by taking literature survey from the previous articles and talk about the cause of the oral detection and the prevalence of Oral cancer in India.

Keywords: Oral cancer, Diagnosis, Morphological features.

1. INTRODUCTION

The lining of the lips, mouth, or upper throat can develop cancer, which is known as oral cancer or mouth cancer. In the mouth, it typically begins as a painless white area that thickens, turns red in spots, develops into an ulcer, and keeps getting worse. It typically appears on the lips as a slow-growing, persistent crusting ulcer that does not heal.

ORAL cancer is a malignant tumour that develops in the tongue, floor of the mouth, hard palate, upper/lower gums, and buccal mucosa. Salivary glands, oropharynx, nasopharynx, and hypopharynx are among the areas affected. The chief signs and symptoms of this condition include recurring or long-lasting ulcers on the oral mucosa, lumps or nodules, discomfort, numbness, and difficulties swallowing. According to reports, cigarettes [1], alcohol, and betel quid, and are the leading oral cancer risk factors. According to certain research, the human papillomavirus [2], and certain dietary habits can both increase the risk of oral cancer. Patients' oral cancer diagnoses are being delayed throughout the world. This is a result of a lack of adequate medical resources. and lack of qualified medical personnel and diagnostic tools. For example, when most patients feel discomfort in the oral cavity, they will contact the family doctor or dental clinic. In many cases, these facilities may not have resources for oral pathological biopsy. This means that only a preliminary oral examination can be done, even though the diagnosis sensitivity highly depends on the doctor's experience. According to a study by Lingen et al., by the time more than 60% of patients were diagnosed, the tumour had progressed to the third and fourth stages. Additionally, the lesion area had reached a size visible to the naked eye [5]. It is estimated that about 80% of patients can live for five years if oral cancer can be detected and located at an early stage [6]–[8]. Therefore, it is necessary to study and develop effective and quick detection methods for early-stage oral cancer and oral precancerous lesion [9]. Meanwhile, cost and portability should also be considered for the detection methods if they are to be promoted and used globally.

A growing body of research on employing artificial intelligence to improve medical diagnostics has been conducted recently (AI). The growing

prevalence of diagnostic imaging has made it possible for researchers to look into the use of AI for the analysis of medical pictures. One AI method in particular, Deep Learning (DL), has demonstrated notable effectiveness in tackling a variety of medical image processing issues [10], particularly in the diagnosis of cancer in pathological images [11]. Computer-Aided Diagnosis (CAD) systems for a variety of cancer types, including breast cancer [12], lung cancer [13], prostate cancer [14], etc., have been suggested and developed on a large scale based on DL. However, the literature shows that DL hasn't been widely used for OSCC diagnosis from pathological pictures. Convolutional Neural Network (CNN) and Random Forest were employed by Dev et al. in a study to identify keratin pearls in images of oral histology. For keratin area segmentation, the CNN model had a 98.05% accuracy rate, while the Random Forest had a 96.88% accuracy rate [15]. Similar to how Das et al used DL to categorise oral biopsy images according to Broder's histological grading scheme, Additionally, CNN was suggested, and it demonstrated a 97.5% classification accuracy [16]. Jonathan et al. used CNN to classify oral cancer tissue into seven categories using Active Learning (AL) and Random Learning (RL) (stroma, lymphocytes, tumour, mucosa, keratin pearls, blood, and adipose). It was discovered that the AL's accuracy outperformed the RL's by 3.26% [17]. Additionally, Francesco et al. divided the whole slide images (WSI) of oral lesions into three classes (carcinoma, non-carcinoma, and non-tissue) using various deep learning architectures, including SegNet, U-Net, U-Net with VGG16 encoder, and U-Net with ResNet50 encoder. A deeper network, like U-Net updated with ResNet50 as the encoder, was demonstrated to have more accuracy than the original U-Net [18]. Recently, Rutwik et colleagues used ResNet to conduct binary classification on pictures of oral disease and reached an accuracy of 91.13% [19].

In this paper, we have researched about various ways to detect oral cancer using AI techniques and image processing in a combination as feature extractors. We also provided a detailed analysis of models' performance using various metrics to report the best network for Oral detection.

2. WAYS OF DETECTION

2.1 Auto-Fluorescence Detection Method for Early-Stage Oral Cancer

This suggests an effective and quick autofluorescence approach for the early identification of oral cancer. The basic automatic equipment prototype with non-invasive detection and real-time observation is built using mechanical composition analysis and 3-D modelling. Using a 560-nm filter with a bandwidth of 30 nm, sublingual gland cysts, herpes simplex, and biological enzyme solutions [flavin adenine dinucleotide (FAD) and nicotinamide adenine dinucleotide (NADH)] at different concentrations are detected. UV-LED light sources at 3 and 5 W with wavelengths of 375, 395, 405, 410, and 420 nm

	Jo et al. [23]	Shaiju et al. [24]	Huang et al. [25]	Lalla et al. [26]	This Work
Method	Multispectral Fluorescence Lifetime Imaging	Spectra Analysis	Auto-fluorescence Detection	Auto-fluorescence Detection	Auto-fluorescence Detection
Output Mode	Fluorescence Lifetime Image	Fluorescence Spectra	Fluorescence Image	Fluorescence Image	Fluorescence Image
Excitation Light Source	Pulsed Laser (355 nm)	Xenon Lamp	UV-LED (400-460 nm)	LED (white light, 405 nm and 545 nm)	UV-LED (375, 395, 405, 410, and 420 nm)
Main Configuration	Pulsed laser + Rigid Endoscope + Fiber + Photomultiplier Tube etc.	Xenon Lamp + Fiber + Spectrofluorometer	VELscope Device	Identafi Device	UV-LED + Fiber + Dichroic Mirror + Emission Filter
Specificity	0.87	0.95	0.923	0.85	0.95

TABLE I

COMPARISON TABLE OF FLUORESCENCE DETECTION METHODS

Additionally, a thorough demonstration of the detecting conditions' applicability to various oral cavity locations is made. Through the use of UV-LEDs with a specified wavelength and observation of the features of lesions, experimental results demonstrate the specificity of 0.95. The suggested detection approach will be useful for auto-detection of precancerous lesions and mouth cancer screening. A range of fluorescence screening techniques for oral cancer are shown in Table I. Jo et al. [21] employed pulsed laser as an excitation method based on multispectral lifetime imaging technology.

photos of the fluorescence lifespan source and collection. The results of the detection revealed a specificity of 0.87. Contrary to autofluorescence technology, the use of photomultiplier tubes to acquire fluorescence signals is slightly insufficient in the visual observation of the lesions, even if fluorescence lifetime images can be utilised to test for oral cancer. Using a Xenon lamp as an excitation light source, Shaiju et al.

A specificity of 0.95 was obtained from spectrometer analysis of the spectra. Contrary to autofluorescence technology, the results' output mode, fluorescent spectra, is unable to represent the lesion's dispersion across a wide field of view or allow for naked eye inspection. Huang et al. [23] employed the VELscope (White Rock), a UV-LED with an excitation light source that has a wavelength between 400 and 460 nm, to analyse the detected pictures. A specificity of 0.923 was attained. Additionally, Lalla et al. [24] achieved a specificity of 0.85 when they performed autofluorescence detection using Identafi (DentalEZ).

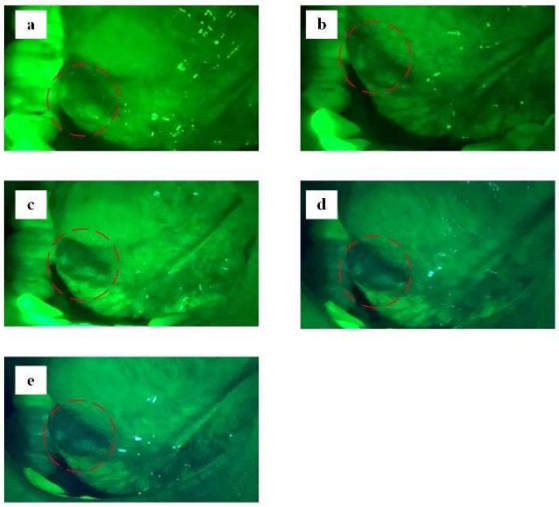

Fig. 1. Auto-fluorescence image of a patient with sublingual gland cyst. (a)–(e) Excited by 3-W LEDs at 375, 395, 405, 410, and 420 nm, respectively.

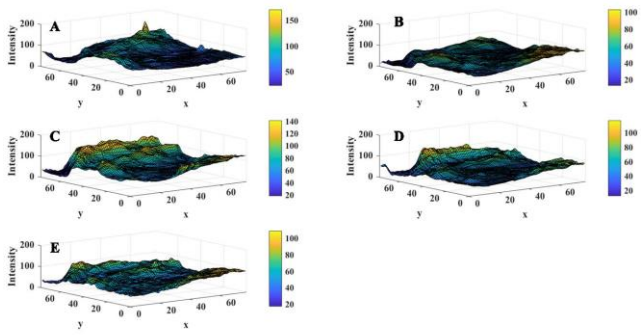

Fig. 2. Color maps of intensity for auto-fluorescence detection image of a patient with sublingual gland cyst. (a)–(e) Excited by 3-W LEDs at 375, 395, 405, 410, and 420 nm, respectively.

photos of auto-fluorescence stimulated by low power LED (see Figs. 1 and 2). The edge of the cyst can be seen clearly, and it is simple to notice that the sublingual gland cyst's lesion area—which is indicated by a red circle—has fluorescence loss under all excitation LEDs. This suggests that the cyst in the sublingual gland is less responsive to the excitation wavelength that is chosen to change. Although the areas of loss are mostly focused around the cyst's periphery, it is still possible to see a few luminous spots in the cyst's bulging upper centre. It is hypothesised that this phenomenon is caused by a shortage of fluorophores in the patient's sublingual cyst's mucus compared with the surrounding normal tissue. Therefore, although the sublingual gland cyst has a noticeable fluorescence loss effect, it can still be distinguished by its unique fluorescence image to reduce the false-positive situation when using the equipment proposed.

2.2 Multisampling Tensor Model for Oral Cancer Classification

Oral cancer and cyst classification from magnetic resonance imaging using an intelligent multisampling tensor model (MRI). In particular, this method first uses four straightforward sampling procedures to encrypt the input image, allowing the model to acquire additional local, global, influential, and correlated information. Next, a representation fusion strategy is used to combine the recovered representations. These are then combined by a series of matrix product states, which perform a classifier operation by mapping the input representation into a high-dimensional space. Finally, they test this suggested approach on data from oral MRI cancer patients, and the experimental finding shows that this strategy could produce competitive classification results.

The overall structure of the proposed multisampling tensor model is illustrated in Fig. 3. The input image first passes through a multisampling layer, and then a series of MPS blocks is utilized to contract the representations into a vector, next we reshape the previous layers' output representations to 2-D

dimension, and repeat those encoding processes until output the final prediction result

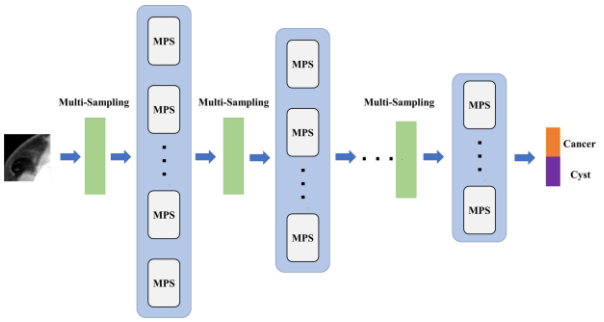

Fig. 3. Overall structure of our designed multi-sampling tensor model. The input image first passes through a multi-sampling layer, and then a series of MPS blocks is utilized to contract the representations into a vector. Next, we reshape the previous layers' output representations to the 2-D dimension and repeat those encoding processes until output the final prediction result.

The traditional tensor network reduces the original 2-D image to a 1-D vector, potentially ignoring its spatial, global, local, and correlative aspects. However, those characteristics might be crucial in the work of classifying oral cancer/cysts. They suggest a straightforward multisampling layer to address this issue, consisting of four sampling operations to encode discriminative characteristics from the input and boost the performance of the model's classification.

I. Local Region Sampling (LRS):

The local regions characterise the visual feature in the oral cancer/cyst classification task with various and specific hints [26]. A local region sampling is used to uncover additional regional traits, which can help extract more diversified representations more effectively. Consider that each feature map's input dimension is H W; the LRS subdivides the entire input into a number of subregions; each subregion is then flattened into a single feature vector, which can represent the local regional characteristics of the entire input. Fig. 4 depicts the LRS operation in detail. The suggested model could encode the regional information from the input subregions using the LRS operation.

II. Average Region Sampling (ARS):

The average intensity of a given region shows the general characteristics of that region and offers more comprehensive information, which may be crucial for the picture classification process. As a result, we apply an ARS operation to each subregion so that it can extract more global and regional properties from the input. Given an input image or feature map with a dimension of H W, we first obey the LRS operation, which separates the entire region into a number of subregions. Then, a ceil average operation is applied to each subregion, resulting in the final output being the ceil average value of each subregion. Fig. 5 depicts the steps involved in carrying out the intended ARS procedure. the global regional characteristics of the input have been well extracted, which can efficiently provide more discriminative representations for the classification task.

III. Max Region Sampling (MRS):

The most influential information in that location is indicated by the region's greatest signal, which typically offers more ethereal representations of the input. We adopt an MRS operation in the multisampling layer, as shown in Fig. 6, in response to that characteristic. Similar to this, after receiving an input, we first partition the entire region into a few smaller parts, as seen in Fig. 7. then after that, a max sampling is carried out, which determines the maximum value of each subregion and uses it as the operation's output. The most important signal of each subregion may be learned through this technique, and it could offer more abstract and significant hints for the feature encoding procedure.

IV. Correlative Region Sampling (CRS):

When learning the high-level and local look of the image, the correlations of the local region are crucial. As a result, we implement a CRS operation in this part to investigate the analogues of each pixel and improve the input's capacity for representation. As shown in Fig. 7, the CRS procedure first separates the image or

feature map into p subregions, following which it calculates the correlative factor vc of each subregion.

$$v_c = \left(\sum_r \sum (d(g,h)) \right) / r \qquad (4)$$

where r is the total pixel numbers of each subregion, d(·) represents the euclidean distance, (g, h) denotes the pixel position of each subregion. Note that the final output vc of each subregion is calculated by averaging the total correlative values of each pixel. By taking account of the correlative representation, the designed tensor model could be more sensitive to the region analogs which further leverage the classification performance.

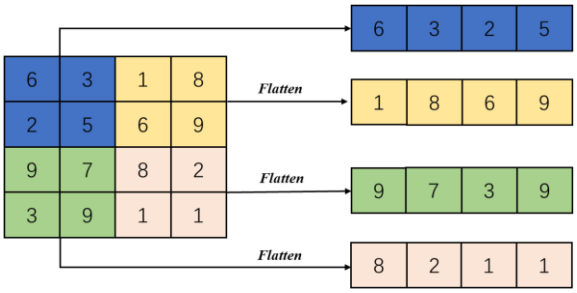

Fig. 4. Process of LRS operation.

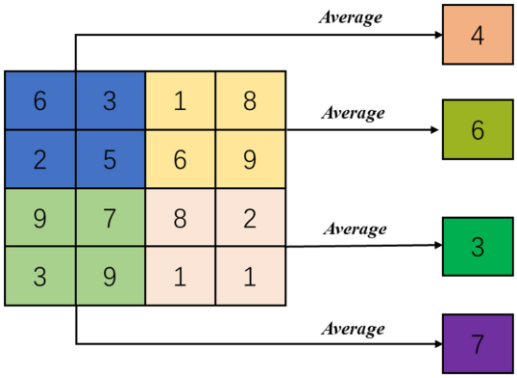

Fig. 5. Process of ARS operation.

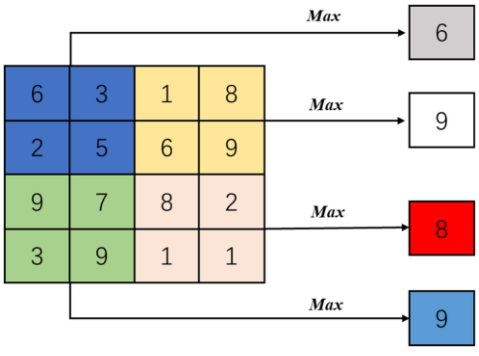

Fig. 6. Process of MRS operation.

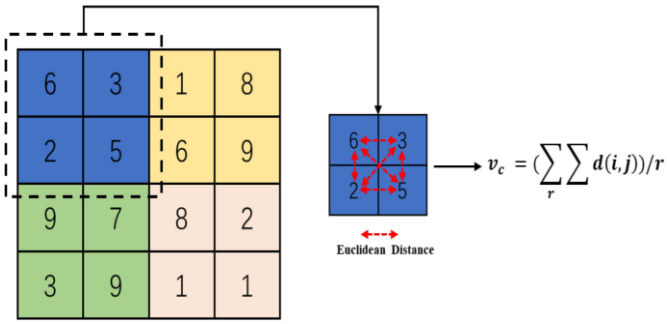

Fig. 7. Process of CRS operation.

A simple multisampling layer is used to learn the local, global, influential, and correlative features from various aspects of the intelligent multisampling tensor model for the classification of oral cancer, and then a representation fusion strategy is used to enhance the performance of the classification model. The final testing findings showed that the suggested model could obtain the best classification performance. To verify its efficacy, they conduct comprehensive experiments using oral MRI data and compare its performance with other ones. Although the experimental findings are competitive on the oral cancer classification job, when transferring it to other medical picture classification tasks, its performance is not as satisfactory as expected. This work's fundamental weakness is that the model's generalisation power is limited.

2.3 Optical Coherence Tomography as an Oral Cancer Screening Adjunct in a Low Resource Settings

The oral mucosa can be non-invasively scanned using optical coherence tomography (OCT), a minimally invasive tomographic imaging technique, to detect premalignant or malignant alteration. The performance of a mobile OCT imaging system as a point-of-care oral diagnostic tool in an LMIC was conceived, built, and evaluated in this study. This pilot study included 20 patients with suspected oral lesions and 10 healthy volunteers. Clinical examination information, a history of risky behaviour, 2-D OCT pictures, and histology were all gathered. Visual grading and calculated image processing methods were used in a blinded evaluation of OCT images for healthy oral mucosa, dysplasia, and cancer. It was found that the OCT image processing

algorithm performed at or exceeded the performance of visual observer scoring of OCT images.

Pre-processing of OCT pictures was required because the probe's spherical and chromatic aberration created imaging abnormalities that led to distorted OCT images (Fig. 8). (a). An edge identification and flattening method was used to fix the deformed shape of the oral mucosa. Using a two-step decision tree, OCT pictures were then categorised as normal, dysplastic, or malignant. Through a comparison of optical tissue stratification, OCT images were initially divided into two categories: non-malignant (normal and dysplastic) vs. malignant. The "non-malignant" group was then classified as either "healthy" or "dysplastic" by looking at changes in the detected basement membrane's deviation at the intersection of the epithelium and lamina propria.

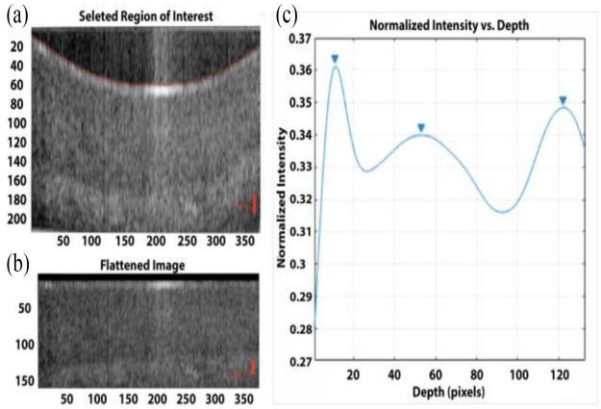

Fig. 8. (a) Edge detection with dynamic programming. (b) Flattened ROI. (c) Smooth depth intensity distribution. Scale bars indicate a length of 106 μm.

When comparing the sensitivity and specificity of other well-established oral cancer screening tests, the diagnostic and screening capabilities of OCT imaging when combined with an image processing algorithm. The conventional oral examination (COE), which employs incandescent light, has long been the accepted standard procedure for screening for oral cancer . Typical sensitivity and specificity values for COE were 85% sensitivity and 97% specificity across numerous large-scale clinical investigations . The image processing algorithm and OCT imaging system employed in this investigation demonstrated superior diagnostic performance to COE. As a result, the suggested OCT-based technique may be used as a supplement to increase the COE's sensitivity and specificity. OCT might not be as helpful in a resource-rich world, though. The best sensitivity and specificity that might be achieved in this situation would be provided by the availability of biopsy and histopathology processing and interpretation. The oral cavity, which has high functionality for speech and swallowing and where tissue preservation is important, can be used to guide clinical decision-making and biopsy. Existing screening procedures for oral cancer frequently employ narrow-mission tissue fluorescence techniques [27]. Their sensitivity is typically far higher than their specificity. The VelScope and Identify [37, 38] systems are two examples of these gadgets. For both systems, the user must draw a personal conclusion from what he or she observes in the fluorescent images. In turn, this necessitates the training of an expert, which limits the device's applicability in remote, underserved, or non-specialist settings.

2.4 Integration of Pathway Knowledge and Dynamic Bayesian Networks for the Prediction of Oral Cancer Recurrence

The current methodology consists of three main steps. In the first step, transcriptomic data are analyzed in order to identify a subset of the most differentially expressed genes among the two groups of patients. In the second step, pathway enrichment analysis is performed for the specific gene list aiming to identify the most significant pathways in terms of overrepresentation. Finally, highly connected genes that participate in the most significant pathways are extracted. This gene list along with the genes determined first as differentially expressed constitute the training set for the development of the interaction networks regarding the prediction of OSCC recurrence. Fig. 9 illustrates the steps followed in the proposed methodology.

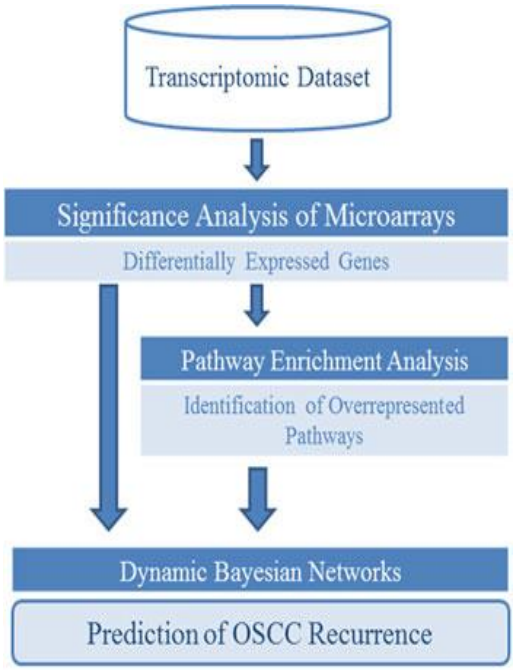

Fig. 9. Schematic representation of the proposed methodology.

In this methodology that exploits transcriptomic data along with pathway knowledge aiming to predict OSCC recurrence through the employment of a DBN algorithm. The obtained results indicate that the integration of time series gene expression data and of distinctly expressed genes among the two groups of patients can provide better knowledge regarding the prediction of a disease relapse. This methodology can be extended to other types of cancer as well as integrate pathway knowledge from various biomedical databases in order to further assess regulatory interactions in a given biological network.

2.5 Multifractal Texture Analysis of Salivary Fern Pattern for Oral Pre-Cancers and Cancer Assessment

Saliva has emerged as an efficient screening sample for early stage detection of oral cancer (OC) owing to non-invasiveness coupled with high sensitivity and specificity. Although spectroscopic characterization of saliva in oral potentially malignant disorders OPMDs) and OC is extensively studied, its potential as imaging biomarker is sparsely explored. Further, the literature on crystalline pattern of saliva for other diseases or different physiological conditions is mostly qualitative.

This article presented a multifractal-based methodology to statistically evaluate salivary fern pattern modification in several OPMDs and OC in comparison to normal counterpart. By using a stereo-zoom microscope in reflecting mode, the fern pattern of dried saliva is photographed, and an image dataset is created. To understand the complexity and heterogeneity of these micro-structured patterns, we turn to two-dimensional multi-fractal detrended fluctuation analysis (2dMFDFA). For the first time, the existence of multifractal nature embedded in salivary fern has been confirmed. The cause of multifractality is discovered to be long-range spatial correlation. Four features taken from the MFDFA show how the multi-scale self-similarity of irregular patterns varies across study groups. The discriminating nature of these features or combinations of pairwise interclass classification is demonstrated by statistical analysis. The acceptability of microscopic images of arborized saliva in quick and economical screening of various oral lesions is clarified by this study.S

Numerous studies have documented alterations in salivary fern structure linked to women's menstrual cycles [31], . Saliva from exclusively male individuals was used in this investigation to reduce this influence. In order to prevent the influence of circadian rhythm on saliva composition, all samples were taken from the patients before breakfast while they were on an empty stomach. One hour before saliva collection, participants were instructed to give their mouths a thorough cleaning with saline water. Thereafter, neither food nor drink was permitted. Before taking images at IIT Kharagpur, a cold chain was maintained throughout the transfer and storage of saliva samples. All participants provided their informed consent before participating in this study, which was also authorised by the institution's ethics committee (GN/ADMN/18/113, dated 09.03.2018).
The samples were initially incubated at room temperature in order to analyse the crystallisation patterns. Each sample's twenty microliters of saliva were poured over a

spotless glass slide. By gradually tilting the slide at an angle of roughly sixty degrees, a thin film of saliva was created. The saliva was allowed to completely dry while the glass slide was kept in a horizontal position. In reflected mode, a stereo-zoom microscope (Olympus MVX10, Olympus Corporation, Japan) was used to analyse the total area of dried saliva films. Using a zoom of 2.5 and a 1x objective (MVPLAPO 1x), a camera attached to the microscope captured microscopic photos with a size of 1358*1024 pixels. Fig. 10 displays representative microphotographs of arborized saliva.

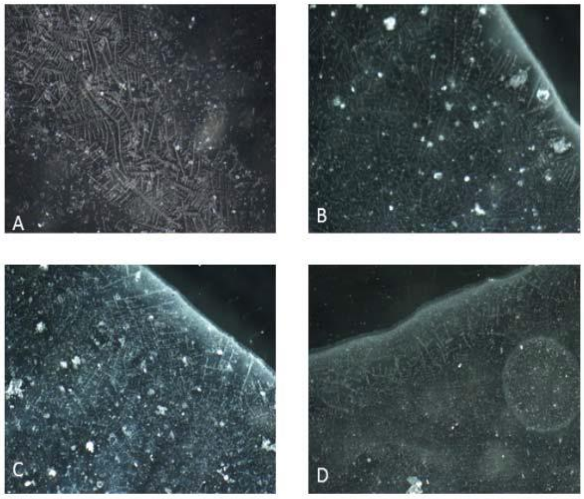

Fig. 10. Microphotographs (25x) of dried saliva for different study groups. (A) NOM, (B) OSF, (C) OLKP and (D) OC.

We have analysed fern pattern of saliva using two-dimensional multifractal detrended fluctuation analysis (2d-MFDFA). Details of 2d-MFDFA can be obtained from [32]

Traditional signal processing methods are unable to distinguish between signals with various scaling behaviours or adequately represent complicated nonlinear signals. In certain situations, fractal analysis can be incredibly useful for gaining novel ideas. Different classes' salivary fern patterns visually resemble one another rather closely. The fern pattern has been studied by the 2d MFDFA in this work, and its multifractal character is acknowledged for the first time. In all study groups, long-range correlation is found to be the cause of the multifractality of the fern pattern. By using extracted 2d MFDFA characteristics, changes to the nonlinear complex fern pattern in OPMDs and OC have been statistically assessed. Student's t test p values show that these characteristics differ statistically significantly between NOM, OPMDs, and OC.Present work illustrated that saliva could provide potential imaging biomarker for early-stage non-invasive diagnosis of OPMDs and OC.

Apart from promising application in the oral cancer diagnosis, present methodology may be applied to study other diseases where crystalline structure of saliva is used to recognize pathological conditions. Further, irregular and self-similar fern pattern of other body fluids viz. tear, blood, cervical mucus can be quantitatively analysed by this method which will be of great value in clinical applications.

2.6 Texture-Map-Based Branch-Collaborative Network for Oral Cancer Detection

In order to automatically detect the ROI and cancerous regions, the article suggests a novel deep convolutional neural network (DCNN) and texture map combination. A lower branch for oral cancer detection and an upper branch for semantic segmentation and ROI marking make up the proposed DCNN model. The upper branch of the network model is used to extract the cancerous regions, and the lower branch improves the accuracy of the cancerous regions. To make the features in the cancerous more regular, the network model extracts the texture images from the input image. Following that, a sliding window is used to calculate the texture image's standard deviation values.. The texture map is then built using the standard deviation values, divided into several patches, and used as the deep convolutional network model's input data.

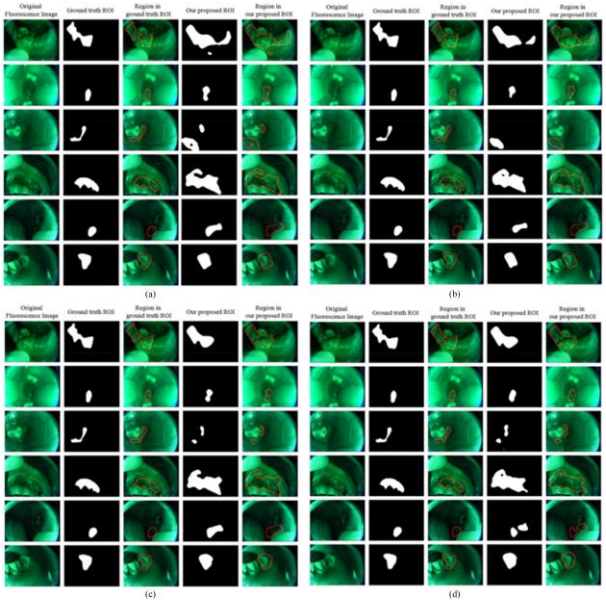

Fig. 11. Cancerous ROIs marked by the resNet + FCN and inception module + FCN architectures. (a) is ROIs marked by FCN architecture based on third level wavelet subband features and resNet (n = 5). (b) is ROIs marked by FCN architecture based on third level wavelet subband features and inception module (n = 5). (c) is ROIs marked by FCN architecture based on Gabor filter features obtained at frequency of λ = 22.2 and resNet (n = 3). (d) is ROIs marked by FCN architecture based on Gabor filter features obtained at frequency of λ = 22.2 and inception module (n = 5).

In this study, we propose a branch-collaborative network based on texture feature images for the identification and ROI marking of cancer in the buccal region of the oral cavity. Wavelet transformation and the Gabor filtering technique have been employed in the suggested model to extract the texture feature images. In order to calculate the associated standard deviation values, a sliding window has therefore been used.

The feature map that was created using the standard deviation values and divided into several patches is then used as the input for the deep convolutional network model The residual network model and the inception module are the two alternative architectures that have been used to implement the oral cancer detection branch. As with the ROI segmentation and marking branch, both a fully convolutional network (FCN) architecture and a feature pyramid network (FPN) architecture[34]. The experimental results have shown that the features extracted by the Gabor filter provide more useful information for the cancer detection and ROI marking tasks than those obtained using the wavelet transformation method. Furthermore, the ROI marking performance for the FCN and FPN designs is comparable. The outcomes have shown that the segmentation branch significantly enhances the proposed model's capacity for ROI marking. Each experiment includes a randomly chosen test set. According to our tests, an average of 70% of the photos have an IOU score that is more than 0.75, which is one approach to gauge how accurately boundaries are matched. It has been demonstrated that lowering the probability threshold used in the detection branch to identify cancer can result in an acceptable trade-off between the suggested model's sensitivity and specificity. The outcomes have demonstrated that the model offers an excellent ability to automatically label the high-risk zones, hence providing a valuable tool for oral cancer screening.

2.7 Automated Detection and Classification of Oral Lesions Using Deep Learning for Early Detection of Oral Cancer

This research presents a novel method for combining bounding box annotations from various doctors. Deep neural networks were also employed to create automated systems from which complicated patterns for completing this challenging task were deduced. Two deep learning-based computer vision approaches—image classification with ResNet-101 and object identification with the Faster R-CNN—were evaluated for the automated detection and classification of oral lesions for the early detection of oral cancer using the preliminary data acquired in this work. The F1 score for image classification was 87.07% for identifying photos with lesions and 78.30% for identifying images that needed to be referred. For the detection of lesions that needed to be referred, object detection achieved a Fl score of 41.18%. Additional performances are presented in terms of classifying in accordance with the referral decision type.

To investigate the job at various levels of difficulty, three different image categorization

models were created (detailed below). In order to produce class confidence scores, the number of neurons in each model's SoftMax classification layer of ResNet-101 was chosen dependent on the number of classes. Fig. 12 shows the multi-class model's general layout.

I. Binary image classification of `lesion' vs. `no lesion'. i.e. `no lesion' vs. the remaining four classes in given data combined to produce the `lesion' class.
II. Binary image classification of `referral' vs. `nonreferral'. i.e. `no lesion' and `no referral needed' combined to produce the `non-referral' class vs. the remaining three classes of Table 4 combined to produce the `referral' class.
III. Multi-class image classification with five classes as detailed from the given data

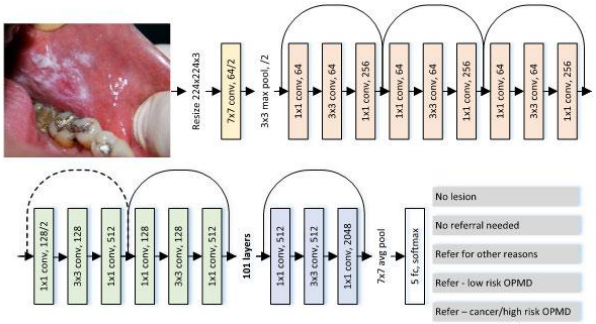

Fig. 12. Outline of ResNet-101 applied to multi-class image classification of oral images. Full details of the ResNet-101 architecture can be found in the original article [36].

In order to investigate the job at various levels of difficulty, three different object detection models were created (detailed below). For each detection, our models report the bounding boxes, the class, and the confidence score. The number of classes was used to determine for each model how many neurons should be included in the SoftMax classification layer of the detection network. Fig. 13 shows the multi-class model's general layout.

I. One object class representing all lesions.
II. Two object classes for the lesions of `referral' vs. `no referral needed'. i.e. `no referral needed' class as detailed in given data vs. the remaining three classes combined to produce the `referral' class.
III. Four object classes with the four referral decision classes for lesions as detailed in given data.

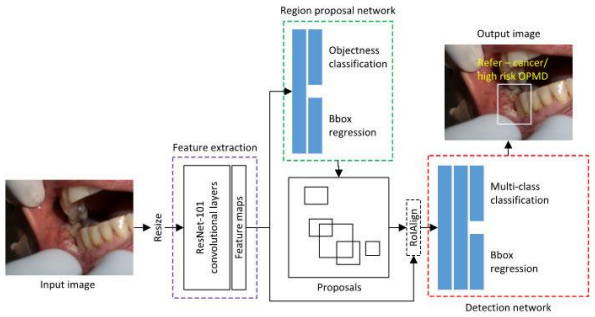

Fig. 13. Outline of the faster R-CNN object detection framework applied to four-class oral lesion detection. Bbox D bounding box.

They have talked about gathering and annotating pictures of the mouth and have shown the outcomes of automating the early diagnosis of oral cancer. They combine the bounding box annotations made by various clinicians, and then they evaluate two various deep learning-based approaches to offer an automation solution. As the dataset expands, performances are expected to improve, which will have a big impact in low- and middle-income countries with scarce health resources.

3. CAUSE

Warning signs and symptoms of oral cancer and associated maxillofacial malignancies

Simple to extremely complicated variations of oral ulcerations may be indicative of oral cancer. In other words, patients typically complain of "ulceration," which refers to damage to the epithelium and connective tissue with the presence of a clear central crater brought on by swelling or growth in the nearby tissue . Medical professionals need to be able to distinguish between reactive lesions that persist for longer than two weeks after the removal of the etiological causes and malignant/premalignant lesions. When these lesions intensify and stop responding to continued treatment, they are considered more suspicious.Therefore, appropriate diagnostic procedures (i.e., gold standard biopsy in addition to other non-invasive chairside procedures of the lesion) are essential diagnostic aids in the evaluation of any lesion

that does not respond to usual therapy in 7 to 14 days . Common oral and maxillofacial

- Non healing ulcer with or without induration / nonhealing socket.
- White patch with firm consistency.
- Red lesion or lesion with erythematous appearance (Erythroplasia).
- Abnormal lump in the mouth with increase in size.
- Exophytic/ulceroproliferative growth.
- Mass or lump in the neck and neigbouring regions (Lymph node enlargement).
- Mobility/ displacement/ non vital teeth/peri implantitis.
- Tooth pain and referral pain.

malignancies presented as persistent non healing oral ulcers are

I. Squamous cell carcinoma – It appears as red or white, painless, indurated, non-healing ulcer with elevated and ill-defined margins. Most of the oral carcinomas may present long standing non-healing ulcero-proliferative lesion with a rolled or indurated border. Common primary tumour sites of the oral cavity as reviewed in literature is attributed to buccal mucosa, tongue, lower alveolus, gingiva, floor of the mouth and palate[38]-[39].

II. Salivary gland tumour - Salivary gland malignancies (muco-epidermoid carcinoma and adenoid cystic carcinomas) occur predominantly in the palate, cheek and gingival region of the jaws as a chronic ulcer [40]-[41].

III. Lymphomas- Lymphomas may present as chronic ulcer covered with necrotic slough in the palatal region of the jaw in specific tumours of palate and paranasal sinus -[42].

IV. Leukemia- Unlike, lymphatic tumours, leukemic tumours occur commonly in the gingival region of the mouth mimicking the clinical picture as lymphomas -.

V. Basal cell carcinoma [43] and Metastatic tumours - may also present as ulcer.

Table 2: Potential warning signs/symptoms of the oral cancer.

4. PREVALENCE OF ORAL CANCER IN INDIA

South and Southeast Asian nations, including India, have the highest rates of oral cancer. Squamous cell carcinoma accounts for 90–95% of mouth cancer cases in India . According to the worldwide agency for cancer research, India would experience an increase in cancer incidence from 1 million in 2012 to more than 1.7 million by 2035. This suggests that the number of cancer-related deaths will likewise rise throughout this time, from 680000 to 1- 2 million. Oral cancer and poor poverty are linked, according to a case-control research from India. Oral cancer growth is influenced by variables such poor diet, inadequate health care, unhealthy living conditions, and risky behaviours.

Oral cancer affects 20 people out of every 100,000 people in India, making up around 30% of all cancer cases. In India, more than 5

persons pass away from oral cancer and the same amount from oropharynx and hypopharynx cancer every hour. Patients in remote locations have poor access to skilled professionals and relatively few health services. As a result, mouth cancer in its advanced stages is mostly to blame for the delay. The best likelihood of long-term survival is with early detection of oral cancer, which also has the potential to enhance treatment outcomes and lower the cost of healthcare. Due to a higher exposure to risk, oral cancer primarily affects those with lower socioeconomic position and those who live in rural areas. due to factors such as use of tobacco

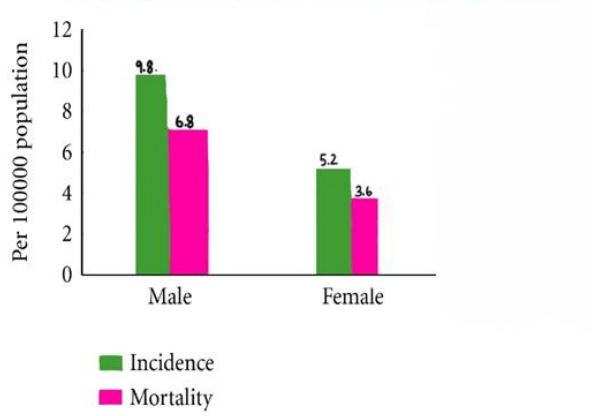

Fig. 14. Incidence and mortality or oral cancer in india

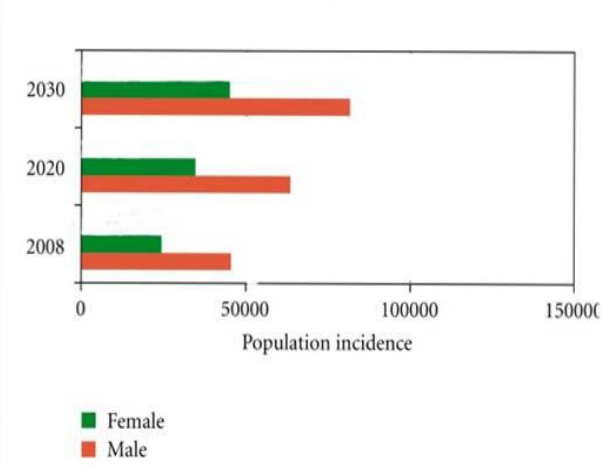

Fig. 15. Incidence in India

Oral cancer affected 53842 men and 23161 women in India in 2012, according to the figures. Oral cancer is thought to be a disease that primarily affects elderly persons. However, the majority of occurrences of oral cancer occur between the ages of 50 and 70, however it can occasionally strike children as young as 10. Oral cancer incidence rises with age. The fifth decade of life is the most typical age. Men are more impacted than women across all age groups when taking gender into account. Men in India are affected by changes in behaviour and lifestyle habits two to four times more than women.

I. Alcohol consumption

Alcohol consumption is a significant mouth cancer risk factor. Risk increases with weekly alcohol use. Alcohol consumption increases the incidence by 49% among current users and by 90% among former drinkers, according to a prospective study conducted in India.

II. Region variation

Additionally, compared to wealthy folks, poor people have a higher age-specific death risk. Tamil Nadu and Kerala, two Indian states, have reasonably decent health outcomes. Future health advancements will be closely related to the country's economic success and collective commitment to fairness and the provision of universal health care. Pan parag, zarda, and other smokeless tobacco products are increasingly popular in north India, particularly in states like Uttar Pradesh. Oral cancer is very common in this area as a result of habit.

III. Use of Tobacco

According to estimates, between the ages of 15 and 49, 57% of males and 11% of women smoke[48]. In more than 90% of OC cases, tobacco use is acknowledged[45]. The use of smokeless tobacco, betel liquid, pan (pieces of Areca nut), processed or unprocessed tobacco, aqueous calcium hydroxide (slaked lime), and certain Areca nut pieces wrapped in Piper betel vine leaf are some of the tobacco consumption methods. Regardless of when they first started chewing tobacco, women who do so 10 or more times per day run a risk that is 9.2 times higher than that of non-tobacco users [45]. In terms of oral dipping products, univariate analysis showed that the risk was 7.3 for consumption of gutka, 5.3 for consumption of chewing tobacco, and 4 for consumption of supari.

Oral cancer can also brought on by poor oral hygiene. More than 85% of patients with oral cancer in one research had bad oral hygiene . In India, the risk associated with poor oral hygiene is approximately 32% for males and 64% for women. Oral cancer was strongly connected with patients who had worn dentures for more than 15 years and who did not regularly see a dentist

While performing routine exams, healthcare professionals should be vigilant for the warning signs and symptoms of oral malignant and premalignant lesions. Recent research revealed variations in the frequency of oral cancer depending on parameters such as age, gender, aetiology, and anatomical sites of occurrence. The importance of prompt clinical evaluation when investigating suspected oral lesions was emphasised by these variables. In order to rule out additional primary malignancies in oral cancer patients, assessments of other possible sites like the oesophagus, larynx, hypopharynx, and lungs should be carried out in addition to the usual clinical and laboratory tests. Although a biopsy is regarded as a confirmatory diagnosis, it is important to validate and increase the clinical applicability of auxiliary advanced diagnostic techniques to detect early malignant tumours

5. CONCLUSION

In this paper, we evaluated the study on the use of several Al methods for the diagnosis of oral cancer disease. Al used an image processing algorithm and mobile image screening to play a key role in the identification of oral cancer. Using the structure of saliva, we can identify a person's pathological condition in addition to predicting oral cancer. Our review article can be expanded to include additional cancer types from different biomedical resources.

REFERENCE

[1] N. L. Rhodus, A. R. Kerr, and K. Patel, "Oral cancer: Leukoplakia, premalignancy, and squamous cell carcinoma," Dental Clinics North Amer., vol. 58, no. 2, pp. 315–340, 2014.

[2] F. Angiero, L. B. Gatta, R. Seramondi, A. Berenzi, and E. Dessy, "Frequency and role of HPV in the progression of epithelial dysplasia to oral cancer," Anticancer Res., vol. 30, no. 9, pp. 3435–3440, 2010.

[3] N. Sharma et al., "Multifractal texture analysis of salivary fern pattern for oral pre-cancers and cancer assessment," IEEE Sensors J., vol. 21, no. 7, pp. 9333–9340, Apr. 2021.

[4] M. Marsden et al., "Intraoperative margin assessment in oral and oropharyngeal cancer using label-free fluorescence lifetime imaging and machine learning," IEEE Trans. Biomed. Eng., vol. 68, no. 3, pp. 857–868, Mar. 2021.

[5] M. W. Lingen, J. R. Kalmar, T. Karrison, and P. M. Speight, "Critical evaluation of diagnostic aids for the detection of oral cancer," Oral Oncol., vol. 44, no. 1, pp. 10–22, Jan. 2008.

[6] N. L. Rhodus, A. R. Kerr, and K. Patel, "Oral cancer: Leukoplakia, premalignancy, and squamous cell carcinoma," Dental Clinics North Amer., vol. 58, no. 2, pp. 315–340, 2014.

[7] C.-H. Chan, T.-T. Huang, C.-Y. Chen, C.-C. Lee, M.-Y. Chan, and P.-C. Chung, "Texture-map-based branch-collaborative network for oral cancer detection," IEEE Trans. Biomed. Circuits Syst., vol. 13, no. 4, pp. 766–780, Aug. 2019.

[8] M. O. Shaikh, C.-M. Lin, D.-H. Lee, W.-F. Chiang, I.-H. Chen, and C.-H. Chuang, "Portable pen-like device with miniaturized tactile sensor for quantitative tissue palpation in oral cancer screening," IEEE Sensors J., vol. 20, no. 17, pp. 9610–9617, Sep. 2020.

[9] G. Banavar et al., "The salivary metatranscriptome as an accurate diagnostic indicator of oral cancer," NPJ Genomic Med., vol. 6, no. 1, pp. 1–10, Dec. 2021.

[10]. F. Altaf, S. M. Islam, N. Akhtar, N. K. Janjua, Going deep in medical image analysis: concepts, methods, challenges, and future directions, IEEE Access 7 (2019) 99540–99572.Google Scholar

[11]. A. Echle, N. T. Rindtorff, T. J. Brinker, T. Luedde, A. T. Pearson, J. N. Kather, Deep learning in cancer pathology: a new generation of clinical

biomarkers, British Journal of Cancer (2020) 1–11.Google Scholar

[12]. A. Duggento, A. Conti, A. Mauriello, M. Guerrisi, N. Toschi, Deep computational pathology in breast cancer, in: Seminars in cancer biology, Elsevier, 2020.Google Scholar

[13]. S. Wang, D. M. Yang, R. Rong, X. Zhan, J. Fujimoto, H. Liu, J. Minna, I. I. Wistuba, Y. Xie, G. Xiao, Artificial intelligence in lung cancer pathology image analysis, Cancers 11 (11) (2019) 1673.Google Scholar

[14]. S. L. Goldenberg, G. Nir, S. E. Salcudean, A new era: artificial intelligence and machine learning in prostate cancer, Nature Reviews Urology 16 (7) (2019) 391–403.Google Scholar

[15]. D. K. Das, S. Bose, A. K. Maiti, B. Mitra, G. Mukherjee, P. K. Dutta, Automatic identification of clinically relevant regions from oral tissue histological images for oral squamous cell carcinoma diagnosis, Tissue and Cell 53 (2018) 111–119.Google Scholar

[16]. N. Das, E. Hussain, L. B. Mahanta, Automated classification of cells into multiple classes in epithelial tissue of oral squamous cell carcinoma using transfer learning and convolutional neural network, Neural Networks 128 (2020) 47–60.Google Scholar

[17]. J. Folmsbee, X. Liu, M. Brandwein-Weber, S. Doyle, Active deep learning: Improved training efficiency of convolutional neural networks for tissue classification in oral cavity cancer, in: 2018 IEEE 15th International Symposium on Biomedical Imaging (ISBI 2018), IEEE, 2018, pp. 770–773.Google Scholar

[18]. F. Martino, D. D. Bloisi, A. Pennisi, M. Fawakherji, G. Ilardi, D. Russo, D. Nardi S. Staibano, F. Merolla, Deep learning-based pixel-wise lesion segmentation on oral squamous cell carcinoma images, Applied Sciences 10 (22) (2020) 8285.Google Scholar

[19]. R. Palaskar, R. Vyas, V. Khedekar, S. Palaskar, P. Sahu, Transfer learning for oral cancer detection using microscopic images, arXiv preprint arxiv:2011.11610 (2020).Google Scholar

[20] auto fluorocent detection

[21] J. A. Jo et al., "Endogenous fluorescence lifetime imaging (FLIM) endoscopy for early detection of oral cancer and dysplasia," in Proc. 40th Annu. Int. Conf. IEEE Eng. Med. Biol. Soc. (EMBC), Jul. 2018, pp. 3009–3012.

[22] S. N. Shaiju et al., "Habits with killer instincts: In vivo analysis on the severity of oral mucosal alterations using autofluorescence spectroscopy," J. Biomed. Opt., vol. 16, no. 8, 2011, Art. no. 087006.

[23] T.-T. Huang et al., "Novel quantitative analysis of autofluorescence images for oral cancer screening," Oral Oncol., vol. 68, pp. 20–26, May 2017.

[24] Y. Lalla, M. A. T. Matias, and C. S. Farah, "Assessment of oral mucosal lesions with auto-fluorescence imaging and reflectance spectroscopy," J. Amer. Dental Assoc., vol. 147, no. 8, pp. 1–11, 2016.

[25] Multisampling Tensor Model for Oral Cancer Classification

[26] R.W. Cutler, "Local region sampling (LRS) : A method to predict protein coding regions," 2020.

[27] D. Roblyer et al., "Comparison of multispectral wide-field optical imaging modalities to maximize image contrast for objective discrimination of oral neoplasia," J. Biomed. Optics, vol. 15, no. 6, Nov./Dec. 2010, Art. no. e066017.

[28] P. Lane, M. Follen, and C. MacAulay, "Has fluorescence come of age? A case series of oral precancers and cancers using white light, fluorescence light at 405 nm and reflected light at 545 nm using the trimira identafi 3000," Gend Med., vol. 9, no. 1 Suppl, pp. S25–S35, Feb. 2012.

[29] Integration of Pathway Knowledge and Dynamic Bayesian Networks for the Prediction of Oral Cancer Recurrence

[30] Multifractal Texture Analysis of Salivary Fern Pattern for Oral Pre-Cancers and Cancer Assessment

[31] E. Lee, I. Kim, H. Nam, H. Jeon, and G. Lim, "Modulation of saliva pattern and accurate detection of ovulation using an electrolyte predeposition- based method: A pilot study," Analyst, vol. 145, no. 5, pp. 1716–1723, 2020.

[32] C. Xi, S. Zhang, G. Xiong, and H. Zhao, "A comparative study of two- dimensional

multifractal detrended fluctuation analysis and twodimensional multifractal detrended moving average algorithm to estimate the multifractal spectrum," Phys. A, Stat. Mech. Appl., vol. 454, pp. 34–50, Jul. 2016.
[33] Texture-Map-Based Branch-Collaborative Network for Oral Cancer Detection
[34] T.-Y. Lin et al., "Feature pyramid networks for object detection," in Proc. IEEE Conf. Comput. Vis. Pattern Recognit., 2017, pp. 2117–2125.
[35] Automated Detection and Classification of Oral Lesions Using Deep Learning for Early Detection of Oral Cancer.
[36] K. He, X. Zhang, S. Ren, and J. Sun, ``Deep residual learning for image recognition," in *Proc. IEEE Conf. Comput. Vis. Pattern Recognit. (CVPR)*, Jun. 2016, pp. 770_778.
[37] Scully C, Porter S .Orofacial disease: update for the dental clinical team: 2. Ulcers, erosions and other causes of sore mouth. Part I. Dent Update. 1998;25(10):478-84.
[38] Yang SW, Lee YS, Chang LC, Hwang CC, Chen TA. Use of endoscopy with narrow-band imaging system in detecting squamous cell carcinoma in oral chronic non-healing ulcers. Clin Oral Investig. 2014;18(3):949-59.
[39] Sharma RG, Bang B, Verma H, Mehta JM . Profile of oral squamous cell cancer in a tertiary level medical college hospital: a 10 yr study. Indian J Surg Oncol. 2012;3(3):250-4.
[40] Zhao C, Liu JZ, Wang SB, Wang SC .Adenoid cystic carcinoma in the maxillary gingiva: a case report and immunohistochemical study. Cancer Biol Med. 2013;10(1):52-4.
[41] Herd MK, Murugaraj V, Ghataura SS, Brennan PA, Anand R 2012.Low-grade mucoepidermoid carcinoma of the palate-a previously unreported case of metastasis to the liver. J Oral Maxillofac Surg. 2012;70(10):2343-6.
[42] Nikolaos N, Gigorios P, Konstantinos k, Savvas T, Vassiliki Z, Alexandra S, et al. Extranodal nasal-type NK/T- cell lymphoma of palate and paranasal sinuses. A J Case Rep. 2012;13:79-85.
[43] Woods TR,Cohen DM,Islam MA,Kratochvi FJ,Reder SL, Bhattacharyya I. Intraoral basal cell carcinoma,a rare neoplasm: report of three new cases with literature review. Head Neck Pathol. 2014;8(3):339-48.
[44] Manisha Sharma1, Manas Madan2, Mridu Manjari3, Tejinder Singh Bhasin4, Spriha Jain5, Saumil Garg6, "Prevalence of Head and Neck Squamous Cell Carcinoma (HNSCC) in our population: The clinicpathological and morphological description of 198 cases"
[45] Sree Vidya Krishna Rao1, Gloria Mejia1, Kaye Roberts-Thomson1, Richard Logan2, "Epidemiology of Oral Cancer in Asia in the Past Decade- An Update (2000-2012)"

[46] Shalini Gupta, Rajender Singh1, O. P. Gupta2, Anurag Tripathi, "Prevalence of oral cancer and pre - cancerous lesions and the association with numerous risk factors in North India: A hospital based study"

[47] Bhawna Gupta1, Anura Ariyawardana2,3 and Newell W. Johnson2 "Oral cancer in India continues in epidemic proportions: evidence base and policy initiatives"International Dental Journal 2013; 63: 12–25

[48] KenRussell Coelho1,2, "Challenges of the Oral cancer burden in India"

[49] SS Rahman1, MK Sarker2, MHA Khan3, SS Biswas4, MM Saha5, "Clinical profile of oral squamous cell carcinoma patients attending a tertiary care hospital"

[50] Johnson NW, Warnakulasuriya S, Gupta PC et al. Global inequalities in incidence and outcomes for oral cancer: causes and solutions. Adv Dent Res 2011 23: 237–246.